# Development of the 15 T $Nb_3Sn$ dipole HD2

P. Ferracin, S. Caspi, D. W. Cheng, D. R. Dietderich, A. R. Hafalia, C. R. Hannaford, H. Higley, A. F. Lietzke, J. Lizarazo, A. D. McInturff, G. Sabbi

***Abstract*— The Superconducting Magnet Program at Lawrence Berkeley National Laboratory (LBNL) is continuing the development of HD2, a 1 m long $Nb_3Sn$ dipole generating a dipole field of 15 T in a 36 mm clear bore. With tilted (flared) ends to avoid obstructing the beam path, HD2 represents a step towards the development of cost effective accelerator quality magnets. The design has been optimized to minimize geometric harmonics and to address iron saturation and conductor magnetization effects. The support structure is based on an external aluminum shell, pre-tensioned with pressurized bladders and interference keys. Aluminum axial rods and stainless steel end plates provide longitudinal support to the coil ends during magnet excitation. This paper reports on field quality optimization and magnet parameters. The design and fabrication of the coil and structure components, and results from coil winding, reaction, and potting are also presented.**

***Index Terms*— $Nb_3Sn$, dipole magnet**

## I. INTRODUCTION

FOLLOWING the successful test of HD1 [1], a 16 T dipole magnet with flat racetrack coils and an 8 mm bore, the Superconducting Magnet Program at Lawrence Berkeley National Laboratory (LBNL) is progressing with HD2 to the next phase of development of block-type coils for accelerators quality magnets. The HD2 conceptual design was described in [2], whereas in [3] a detailed mechanical analysis of structure and coil was reported. In this paper, we present the final HD2 lay-out, with particular emphasis on the components optimized to achieve high field homogeneity. The planned assembly and loading procedures, with the status of the fabrication of structure and coils, are also discussed.

## II. MAGNET DESIGN AND PARAMETERS

Each of the two coil modules of HD2 (Fig. 1) is composed of two layers wound from a continuous length of cable made of 51 strands with a 0.8 mm diameter (see Table I for the cable parameters). Layer 1, with 24 turns, is wound around a titanium alloy (Ti 6A-4V) winding pole which features a round cutout to provide room for the bore tube. Layer 2, with 30 turns, is wound around another solid titanium alloy pole. The two coils are separated by a stainless steel mid-plane sheet 1.37 mm thick, and assembled around a 3.65 mm thick stainless steel (Nitronic 40) bore tube with a clear aperture of 36 mm.

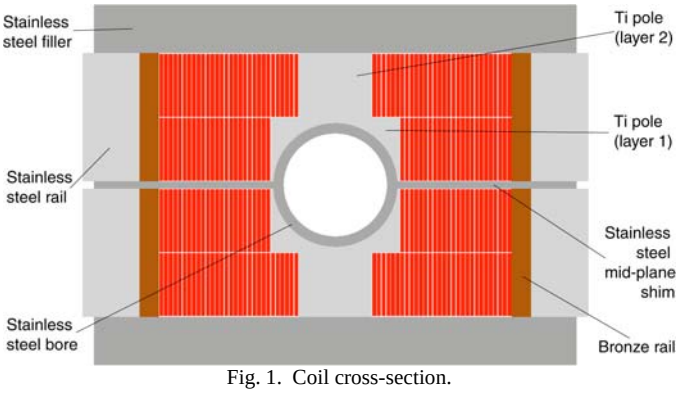


Fig. 1. Coil cross-section.

Aluminum-bronze and stainless steel side rails are placed in between the conductors and the horizontal pads (see Fig. 2), whereas the volume between the coil and the vertical pads is filled with a sub-assembly composed of a stainless steel filler, an iron insert and two stainless steel inserts. Two yoke halves, made of 50 mm thick iron laminations, and a 41 mm thick aluminum shell provide the external coil pre-load through vertical and horizontal interference keys. The diameter of the cold mass is 705 mm. Magnet parameters are given in Table I: assuming HD1 strand properties, the magnet generates a maximum bore field of 15.0 T (4.2 K), with a conductor peak field of 15.8 T. The magnet's short sample limits will be updated according to the measurements of witness strand samples reacted with the coils.

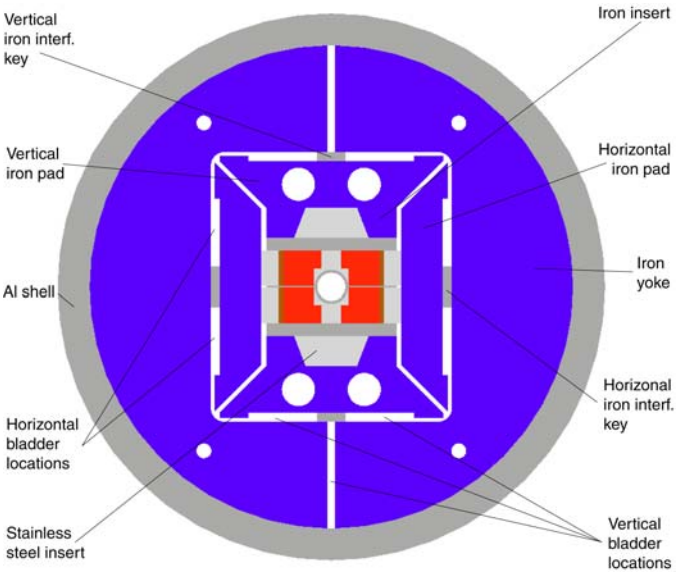


Fig. 2. HD2 cross-section.

Manuscript received August 28, 2007. This work was supported by the Director, Office of Energy Research, Office of High Energy and Nuclear Physics, High Energy Physics Division, U. S. Department of Energy, under Contract No. DE-AC02-05CH11231.

All authors are with Lawrence Berkeley National Lab, Berkeley, CA 94720 USA (phone: 510-486-4630; fax: 510-486-5310; e-mail: pferracin@lbl.gov).

TABLE I MAGNET DESIGN PARAMETERS

| Parameter | Unit | |
|---|---|---|
| Strand diameter | mm | 0.8 |
| No. strands | | 51 |
| Cable width (bare) | mm | 22.000 |
| Cable thickness (bare) | mm | 1.400 |
| Insulation thickness (h/v) | mm | 0.110/0.110 |
| No. turns/quadrant (layer 1) | | 24 |
| No. turns/quadrant (layer 2) | | 30 |
| Short sample current | kA | 17.3 |
| Maximum dipole field | T | 15.8 |
| Coil peak field | T | 15.0 |
| Stored energy | MJ/m | 0.84 |
| Inductance | mH/m | 5.6 |
| Fx / Fy layer 1 (per quadrant) | MN/m | + 2.3 / - 0.3 |
| Fz layer 1 (per quadrant) | kN | 90 |
| Fx / Fy layer 2 (per quadrant) | MN/m | + 3.3 / - 2.2 |
| Fz layer 2 (per quadrant) | kN | 126 |

An overview of the 3D coil and magnet designs is shown in Fig. 3. The coil has a straight section of 481 mm and 475 mm, respectively in layer 1 and 2, and it tilts up (flares) at a $10^{o}$ angle in both ends through hard-way bends, whose minimum radius is 349 mm at layer 2. After the hard-way bends, the flared region features a short straight section of 117 mm in layer 1 and 135 mm in layer 2.

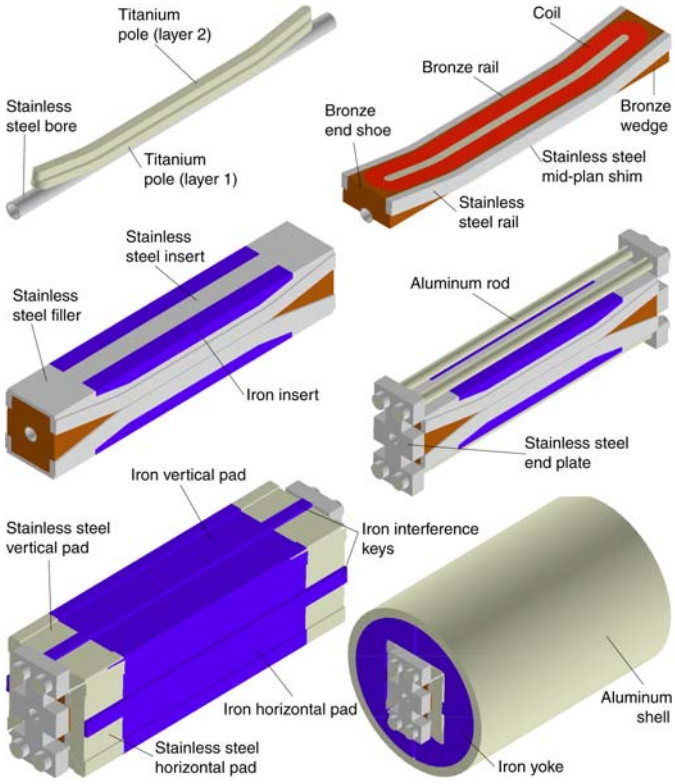


Fig. 3. HD2 3D design.

The tilted ends are vertically supported by aluminum-bronze wedges surrounding the bore tube. The coil sides are then constrained by aluminum-bronze rails which, along with the end-shoes, enclose and define the coil envelope. Stainless steel rails transfers the horizontal pre-load from the pads to the conductors (no horizontal force is transferred to the wedges or to the mid-plane shim).

The volume delimited by the coil and the vertical pads is filled by three components: a stainless steel machined plate (filler), which covers the entire top surface of the coil's second layer, a stainless steel insert, which transfers the vertical load from the pads to the coil in the straight section, and two an iron inserts, whose shape has been designed to minimize the effect of iron saturation on field quality. Both the vertical and horizontal pad sub-assemblies are composed of one iron segment and two stainless steel segments, whose axial lengths was chosen to reduce field and stresses in the coil ends. In the end regions, 50 mm thick stainless steel endplates (Nitronic 40), connected by four 18.5 mm diameter aluminum rods, constitute the coil axial support system.

## III. ASSEMBLY AND LOADING PLAN

As a first step of the magnet assembly, the yoke laminations will be inserted in the shell. Bladders will be pressurized in between the yoke gaps to spread the yokes apart and insert yoke gap keys. After bladder deflation, the keys will lock the generated clearance, thus ensuring tight contact between laminations and shell. The second step will consist in bolting the pads around the two coil modules, stacked together with the bore tube and the mid-plane shim. After the insertion of the coil-pad sub-assembly in the yoke-shell sub-assembly, a second loading operation will be performed, this time using bladders placed between pads and yoke. By pushing the yoke against the shell and compressing the coil pack, the bladder pressurization will allow removing of the yoke gap keys and inserting of the interference keys. This represents an intermediate loading operation aimed at pre-loading the coil-pack. As a next step, the axial support system will be assembled and pre-loaded with a hydraulic tensioning fixture. Finally, bladders will be inserted between horizontal pads and yoke and in between the yoke gaps for the final pre-tensioning of the shell. We refer to [3] for a mechanical analysis of the stress in coil and structure from assembly to excitation.

## IV. MAGNETIC ANALYSIS

The coil and iron designs were optimized to minimize geometric harmonics, magnetization and saturation effects, at the same time enhancing the bore field in the straight section while lowering the peak field in the ends. The following solutions have been implemented to reduce the end field: in addition to the increasing distance between coils at the tilted ends, a relative longitudinal shift of about 15 mm was applied between the two layers along the flare angle. In addition, non-magnetic parts were included in the vertical and horizontal pads. The impact of iron saturation on magnetic field was reduced by including stainless steel rails 22 mm thick between the coil and the horizontal pad, and by including in the design trapezoidal-shaped iron inserts on top of layer 2. To address the effect of persistent current on field quality, an iron ring 0.3 mm thick, placed in contact with the inner surface of the bore tube, was investigated as a possible correction scheme (as proposed in [4]). In Fig. 4 and Fig. 5, the computed harmonics $b_3$ and $b_5$ for a reference radius of 10 mm are shown as a function of the magnet current.

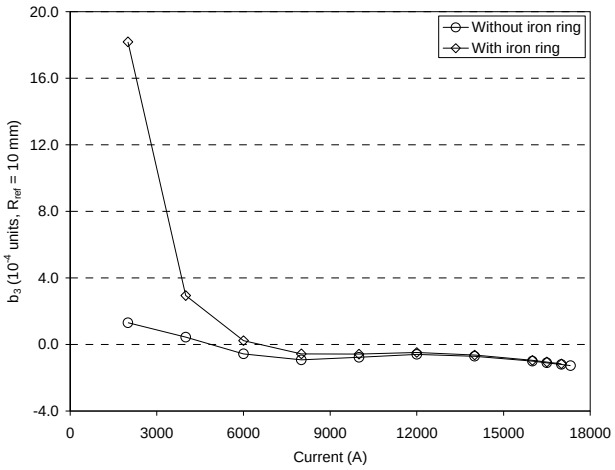


Fig. 4. Computed $b_3$ ($10^{-4}$ units at a $R_{ref}$ = 10 mm) as a function of I (A).

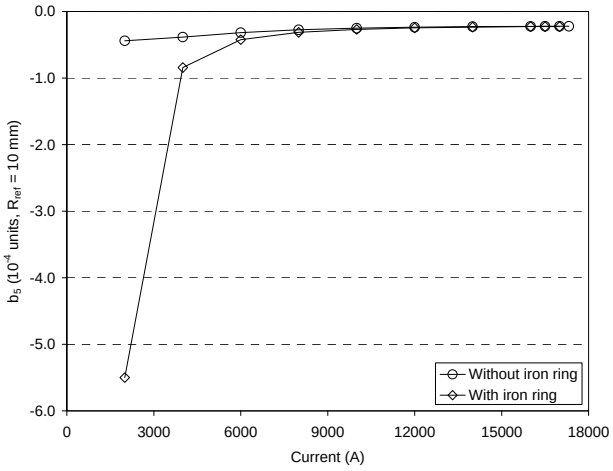


Fig. 5. Computed $b_5$ ($10^{-4}$ units at a $R_{ref}$ = 10 mm) as a function of I (A).

In the current range of 2-17 kA, the $b_3$ varies within ± 1.3 units, while the $b_5$ changes from -0.4 to -0.2 units. The corrective iron ring produces a significant variation in the two harmonics at low field, resulting in a partial compensation of the expected magnetization effect [5]. Further computations and field quality optimizations will be performed based on the final design of the coil ("as built") and on the measurements of the persistent current effects.

## V. Coil and Structure Fabrication

At the time of submission of this paper, all the components of the support structure (shell and yoke laminations in Fig. 6) and coil parts have been fabricated. A fully reacted and impregnated practice coil was completed. Presently, the first HD2 coil module has been wound and reacted.

### *A. Conductor and cable*

The superconducting cable was fabricated and insulated at LBNL using Oxford Superconducting Technology (OST) strands formed by the 54/61 sub-element Restacked Rod Process (RRP) [6]. The critical current density at 4.2 K and 12 T ranges from 2800 to 3000 A/mm$^2$. Cable parameters (see Table I) were optimized to ensure mechanical stability during coil winding.

### *B. Coil winding*

The coil winding starts with layer 2, using the stainless steel filler, in an upside down position, as a winding base. Stainless steel side extensions are bolted on to the sides of the filler to facilitate the clamping and pre-loading of the coil for reaction. After covering the filler with a 0.250 mm thick sheet of fiberglass, the layer 2 pole is installed on the filler and secured with pins and bolts. 30 turns are then wound at a cable tension of 200 N, starting from the layer-to-layer ramp. Voltage taps are installed, mostly in pole turn, as the winding operation proceeds.

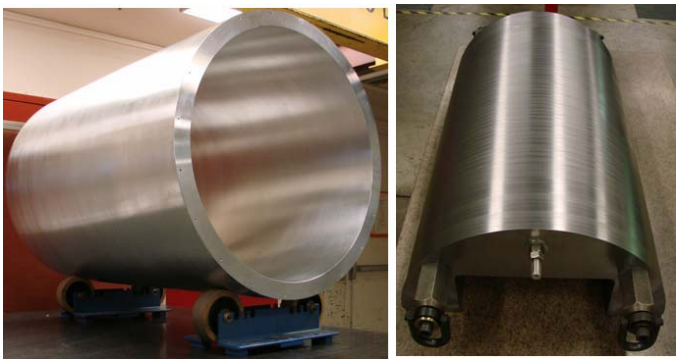

Fig. 6. Aluminum shell and iron yoke laminations.

Once the layer is completed (see Fig. 7, left), end shoes and aluminum-bronze rails are placed around the outer turns and the entire layer is clamped with side pushers. After covering layer 2 with three fiber glass sheets (0.25 mm thick) in the flared regions and 1 sheet in the straight section, the layer 1 pole is interlocked with the layer 2 pole via machined-in longitudinal key/keyway features. 24 turns are then wound from the remaining length of $Nb_3Sn$ cable (see Fig. 7, right). The layer 1 end shoes and side rails are then installed and clamped with side pushers.

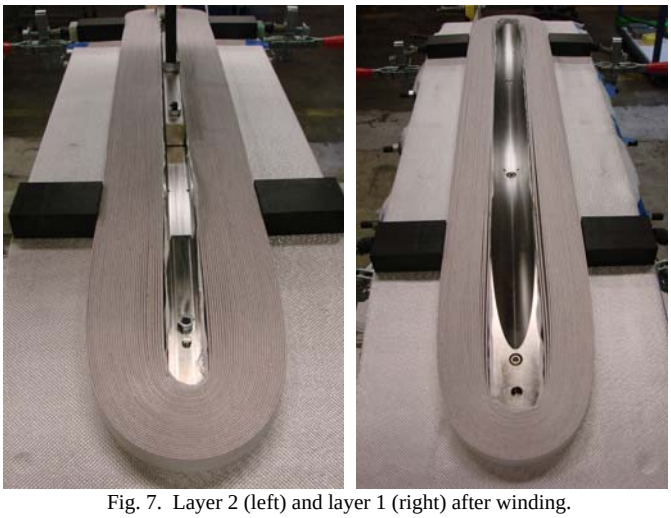

Fig. 7. Layer 2 (left) and layer 1 (right) after winding.

At this point, the aluminum-bronze wedges and the stainless steel mid-plane shims are assembled, and the whole pack is clamped vertically by the reaction fixture top plate (see Fig. 8) and horizontally by two bolted side plates. Stainless steel shims between the coil and the side rails, inserted during the winding process, maintain a 3-4 MPa pressure on the coil when the reaction fixture is bolted closed.

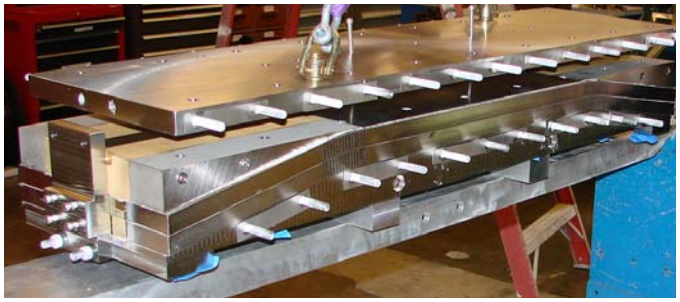

Fig. 8. Reaction fixture.

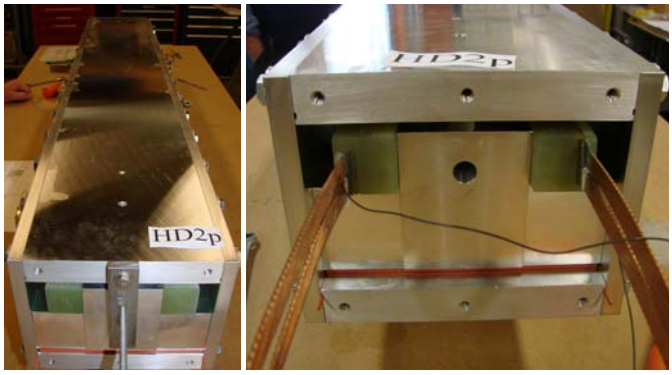


Fig. 9. Impregnation fixture.

Stainless steel posts are attached to the lead end shoe to support the leads during reaction. To hold the end shoes in place along the axial direction, two small end pushers are bolted to the fixture extremities. The reaction fixture is then placed inside the reaction oven for heat treatment.

### C. Heat treatment and epoxy impregnation

The coils are reacted in argon atmosphere according to the following heat treatment schedule: 210 °C for 72 h, 400 °C for 48 h, and 665 °C for 48 h. To facilitate distribution of argon gas for during reaction, the filler, pole, and wedge designs incorporate groove and passage features. After reaction, the fixture is disassembled, and the mid-plane shim, the wedges, and the layer 1 and 2 lead end shoes are removed to expose layer 1 and the outer turns of both layers. Dual NbTi leads are soldered to the out-going $Nb_3Sn$ leads; the lead end shoes are reinstalled after the stainless steel reaction posts are replaced by identical G-10 posts. These posts support the soldered joint as well as the instrumentation trace where the instrumentation wires are soldered. The trace, with integrated quench protection heaters and routes for bringing the voltage tap signals out, is placed on the layer and soldered to the taps.

After reinstalling the wedges and the mid-plane shim, the inner aluminum potting plate is assembled and bolted onto the rest of the assembly. This assures that the reacted coils are fully clamped and supported during the roll-over process to remove the layer 2 reaction fixturing. Next, the same operation is repeated for layer 2, with the soldering of the trace to the voltage taps after the removal of the stainless steel filler. The layer 2 trace design integrates the route for five voltage taps and the quench protection heaters, with in addition two strain gauges mounted on the pole and a spot heater. The stainless steel filler is reinstalled and an outer aluminum potting plate is placed on the assembly. Aluminum side plates are bolted onto the edges of the inner and outer potting plates.

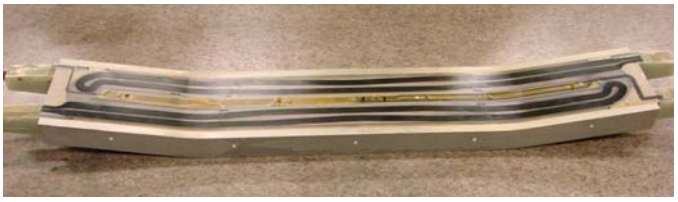

Fig. 10. Practice coil.

Teflon and aluminum end fillers are assembled at the lead and return ends of the end shoes to fill in the cavities. All the aluminum potting plates have machined o-ring grooves which are filled with rubber o-ring material with RTV sealant to prevent leakages. This completes the assembly of the impregnation fixture. The whole impregnation fixture assembly is then vertically placed in a support frame on its return end, and sealed in the impregnation vacuum chamber. Each of the four aluminum side plates has stainless steel strip heaters on each face. The chamber is pumped down to vacuum and the strip heaters are hooked up and controlled to heat the impregnation fixture over night to remove any moisture. A controlled flow of epoxy from a heated mixing pot outside the chamber at ambient pressure is introduced from bottom to top in the impregnation fixture while the chamber is under vacuum. The slow-fill process takes about four to five hours. After filling, the strip heater controller is set to ramp up the impregnation fixture temperature in order to cure the epoxy over night. When the curing is completed, the aluminum impregnation fixture plates are removed and the hardened epoxy films and filler pieces at the coil ends are carefully cleaned up from around the coil assembly. Fig. 10 shows the potted practice coil at the end of the cleaning process.

## VI. Conclusions

HD2 is a 15 T $Nb_3Sn$ block-type dipole with a bore of 36 mm and flared ends. The supporting structure, based on an external aluminum shell, is assembled and loaded with pressurized bladders. The coil cross-section and the iron components have been optimized to correct geometric and saturation field harmonics. A strategy to partially correct the effect of persistent currents on magnetic field has been analyzed. The fabrication of the support structure and one practice coil has been completed. Presently, the fabrication of the two HD2 coils is under way. Final assembly and test are expected to be performed at LBNL in the coming months.

## References

[1] A. F. Lietzke, *et al.*, "Test results of HD1b, an upgraded 16 T $Nb_3Sn$ dipole magnet", *IEEE Trans. Appl. Supercond.*, vol. 15, no. 2, June 2005, pp. 1123-1127.

[2] G. Sabbi, *et al.*, "Design of HD2: a 15 T $Nb_3Sn$ dipole with a 35 mm bore", *IEEE Trans. Appl. Supercond.*, vol. 15, no. 2, June 2005, pp. 1128-1131.

[3] P. Ferracin, *et al.* ,"Mechanical design of HD2, a 15 T $Nb_3Sn$ dipole magnet with a 35 mm bore", *IEEE Trans. Appl. Supercond.*, vol. 16, no. 2, June 2006, pp. 378-381.

[4] S. Caspi, LBNL Internal Note, SC-MAG-691, October 1999.

[5] L. Chiesa, *et al.*, "Magnetic field measurements of the $Nb_3Sn$ common coil dipole RD3c", in *Proc. 2003 Particle Accelerator Conference*, Portland, OR, 2003, pp. 170–172.

[6] S. Hong, *et al.*, "[8] Latest Improvements of Current Carrying Capability of Niobium Tin and Its Magnet Applications" *IEEE Trans. Appl. Supercond.*, vol. 16, no. 2, June 2006, pp. 1146–1151.